AXOPLASMIC TRANSPORT IN THE CRAYFISH NERVE CORD

The Role of Fibrillar Constituents of Neurons

H. L. FERNANDEZ, P. R. BURTON, and F. E. SAMSON

From the Department of Physiology and Cell Biology, The University of Kansas, Lawrence, Kansas 66044

ABSTRACT

(*a*) Axoplasmic transport of tritium-labeled proteins in crayfish nerve cord was confirmed at a slow rate of 1 mm/day. A second proteinaceous component which moves at a rate of 10 mm/day was also detected. Radioautography and biochemical analysis indicate that proteins migrating at these velocities have a perikaryal origin and move caudad within axons as sharply defined peaks. (*b*) Evidence is presented for the blockage of the slow and the fast movement of proteins by intraganglionic injection of the antimitotic agent vinblastine sulfate (0.1 mM). (*c*) Electron microscope observations of vinblastine-treated ganglia revealed a reduction in the number of axonal microtubules and the formation of intracellular aggregates presumably composed of microtubular protein. (*d*) These findings would be compatible with the involvement of microtubules in both slow and fast axoplasmic transport. However, the block induced by vinblastine was detected in regions of the cord (up to 10 mm away from the injection site) where the number and morphology of microtubules appeared unaltered. In addition, axons showing effects of vinblastine occasionally contained mitochondria with remarkably dense and thickened membranes. (*e*) In association with the surfaces of axonal microtubules are lateral filamentous elements (40–80 A in diameter) which also showed vinblastine-induced alterations. Our observations indicate that such filiform structures, associated with microtubules, may be a necessary component in the transport mechanism(s).

INTRODUCTION

Part of the cytoplasm of vertebrate and invertebrate neurons is transported continuously along the axon at 1–3 mm/day (1). Faster movements of proteins, vesicles, and other particulates also occur in the range of 10–2800 mm/day (2). These findings have been confirmed in a variety of nerve cells of mammals, birds, and amphibia by many investigators (1–3).

The mechanisms underlying these transport phenomena remain obscure because the precise ultrastructural basis of axonal transport is unclear; for example, are both slow and fast transport mediated by the same or by different systems? In the case of rapid transport, microtubules or neurofilaments in a neuron have been postulated as the translocating structures (4, 5). The slow movement of materials has been suggested to be a consequence of microperistaltic pressure waves in the axolemma (1). Recently, several papers have shown that colchicine, which selectively binds to

microtubule protein (6, 7), can block fast (8–10) and slow transport in neurons (11, 12). These observations suggest that both transport systems are intimately linked and may depend on the microtubular complex in the axon.

Earlier experiments by Dr. Fernandez showed that colchicine and cold (3°C), which also interferes with the structure of certain microtubules (13, 14), block the slow movement of proteins in the crayfish nerve cord (12). In both instances, normal-appearing microtubules were observed by electron microscopy. Hence, the involvement of microtubules in slow transport could only be inferred, from these experiments, by assuming that both treatments had not dissociated but had inactivated microtubules.

Since it is uncertain whether microtubules participate in axonal transport, we have given further consideration to the role of fibrillar constituents of neurons in such activities. In this paper, we report the effects of vinblastine sulfate, an alkaloid that binds to microtubular protein (15, 16), on the rapid and the slow transport of proteins in the crayfish ventral nerve cord.

MATERIALS AND METHODS

Injection Procedure

3–5-inch crayfish, *Procambarus clarkii girard*, 25–35 g, from the Lemberger Co. (Oshkosh, Wis.), were maintained in aerated aquaria in shallow tap water at room temperature and fed daily.

Injections were made directly under the epineurium of one of an animal's abdominal ganglia through a 2-μ tipped pipette, 0.3 μl of Van Harreveld saline, buffered at pH 7.6, containing either 0.9 μCi of L-leucine-^{3}H (60 Ci/mmole) (Schwarz Bio Research, Inc., Orangeburg, N. Y.) or 0.1 mM of vinblastine sulfate (Eli Lilly & Co., Indianapolis, Ind.) was injected. Sufficient bromophenol blue (Fisher Scientific Co., Pittsburgh, Pa.) was added for the purpose of monitoring visually the progress of the injection.

The microinjection technique, methodology controls, sampling of tissue, and liquid-scintillation counting of the radioisotope incorporated into trichloroacetic acid (TCA)-precipitable protein in the nerve cord have been described previously (17).

Vinblastine sulfate, an alkaloid obtained from the periwinkle plant *Vinca rosea*, dissociates mitotic microtubules and also binds to microtubular protein, particularly that of nervous tissue (15, 16). Since this agent also interferes with cellular metabolism (18), preliminary tests were performed with vinblastine administered to a ganglion that had been previously injected with leucine-^{3}H. In eight animals, different time intervals were allowed between injections, and incorporation of the radioisotope was monitored after 12 hr. These controls showed normal incorporation following injections more than 3 hr apart. In all subsequent experiments, the alkaloid was administered (to a different ganglion) at least 8 hr and usually 24 hr after the injection of the labeled precursor. Hence, the possible interference of this drug with the synthetic mechanisms of the nerve cells could not affect the outcome of our experiments.

The behavior and response to tactile stimulation of all crayfish treated with vinblastine for up to 19 days could not be distinguished from that of untreated animals.

Electrophysiological Procedure

Neural activity was measured, in vitro, by carefully dissecting out the length of the cord, free from the abdominal artery, from the first to the sixth abdominal ganglion. The cord then was placed, over platinum electrodes 3 mm apart, in a small moist plexiglass chamber containing Van Harreveld solution at room temperature.

Supramaximal stimulating shocks (0.1–0.3 msec) with a 5/sec repetition rate from a Tektronix 161 pulse generator (Tektronix, Inc., Beaverton, Ore.), connected through an isolation transformer to platinum electrodes, were applied near the proximal end of the nerve cord. The propagated action potentials were monitored externally by a second pair of platinum wires placed at the distal end of the cord, connected to a Tektronix FM-122 preamplifier and to a Tektronix 532 oscilloscope.

Stimulation and recording of the bioelectric potentials was made every 15 min by lowering the level of saline in the chamber for 1 or 2 min in order to avoid the shortcircuiting factor of the solution. Control tests with the nerve cord maintained as described above showed that the neural activity does not change significantly for up to 24 hr or more.

The effect of vinblastine (0.1 and 0.2 mM) was tested for up to 8 hr by replacing the saline solution in the chamber by the drug. As it was not known if the epineurial sheath in the crayfish cord was permeable to vinblastine, the drug was also injected through the epineurium into one or two adjacent ganglia before recording. Long term experiments were performed by injecting the drug in vivo and monitoring the nerve cord electrical activity 5 and 8 days after the injection.

Electron Microscopy

The electron microscope was used to examine cords 20 min, 60 min, and 4, 8, and 19 days after the intraganglionic injection of 0.1 mM of vinblastine in saline

solution. Although other concentrations were used, best results were obtained with 0.1 mM vinblastine.

For controls, cords of other crayfish were similarly injected with only saline solution. Injected ganglia and adjacent regions of nerve cords were fixed at room temperature for 1–5 hr with either a paraformaldehyde-glutaraldehyde fixative (19) or 2–3% glutaraldehyde buffered with 0.1 M cacodylate at pH 7.4. Both sucrose (20) and 1.0 mM of calcium chloride were added to the fixative. After fixation, samples were washed overnight in three changes of cold buffer and postfixed for 30 min–1 hr in 1% OsO_4 buffered with *s*-collidine (21) or cacodylate at pH 7.2–7.4. After postfixation, the material was dehydrated through an ethyl alcohol series to propylene oxide, then embedded in Epon 812. Sections were picked up on grids coated with Parlodion and a thin film of amorphous carbon, and stained with lead citrate (22) and saturated (aqueous) uranyl acetate.

Samples were examined with an RCA EMU-3H electron microscope, and for purposes of critical measurements the microscope was calibrated using carbon-grating replicas.

Radioautography

In these experiments, 0.3 μCi of leucine-^{3}H in 0.3 μl of saline solution were used for the injections.

The segments to be radioautographed were fixed in a manner identical with that outlined above, and subsequently embedded in paraffin. Longitudinal and transverse sections 5–7 μ thick were mounted on glass slides and allowed to dry after removal of paraffin with xylene and passage through alcohols and distilled water. The sections were then coated either with Kodak NTB-2 or with Ilford L-4 nuclear emulsion (Ilford, Essex, England) (23). Exposure of the samples was carried out in a light-tight box in a desiccator at 4°C for periods ranging from 3 to 12 wk. After development, specimens were stained through the emulsion with methylene blue–azure II and examined under a Zeiss optical microscope.

For testing the possibility that free leucine-^{3}H might migrate along the cord by pathways other than axonal transport, or that our observations were the result of a local synthesis occurring in the axons, injections were made into segments of the cord between adjacent ganglia. In these controls, no significant amounts of labeled proteins were found in longitudinal sections made 1 or more days after injection.

Free leucine-^{3}H was effectively washed out of the tissue by the fixation and dehydration procedures of radioautography. This was checked by assaying the total radioactivity in 1 mm serial sections of nerve cord prepared for radioautography. Nerve cords treated in this manner showed radioactivity patterns identical to those obtained for leucine-^{3}H incorporated into TCA-insoluble protein.

RESULTS

Axonal Transport Rates

The distribution of protein-bound radioactivity in 1-mm segments of nerve cord was followed from 6 to 36 hr after the injection of leucine-^{3}H. A sharp peak of radioactivity incorporated into TCA-precipitable proteins was always detected traveling caudad at 10 ± 1 mm/day. This movement of tritium-labeled proteins was measured in 19 experiments, of which a representative set is illustrated in Fig. 1. 24 hr after injection of leucine-^{3}H a second peak was detected migrating distally and representing slow transport. Longer intervals between injection and biochemical analysis further exaggerate the distance between slow and fast peaks. In long-term experiments, when 1–19 days are allowed to elapse between injection and cord removal, the slow peak is found to move at a rate of 1.1 ± 0.2 mm/day as has been reported previously (17).

Radioautography

In ganglia fixed 1 hr after injection of the labeled precursor, silver grains were seen mainly over cell bodies of neurons. It was observed that intense localization of silver grains occurred over perikarya in which the amino acid was incorporated into protein, and the relative absence of grains over surrounding tissue further indicated (see Materials and Methods) that free amino acid was satisfactorily washed out of the tissue sections (Fig. 2). As the time between injection and cord removal was increased, the number of grains over the perikarya decreased and the label over the axons increased dramatically, whereas the number of background grains remained relatively constant.

Two fractions of the protein-bound label moving distally along the axons, at estimated rates of 1 mm/day and 10 mm/day, were detected in radioautographs from longitudinal sections made at several time intervals after injection (Fig. 3). These rates were resolved by taking the distances from the caudal end of the injected ganglion to the leading edge of each labeled component and dividing them by the injection-to-death elapsed time. The precise localization of the cell bodies in the ganglion was not known; however, no cell bodies are present at the output end of the ganglion, therefore, the rates calculated above must

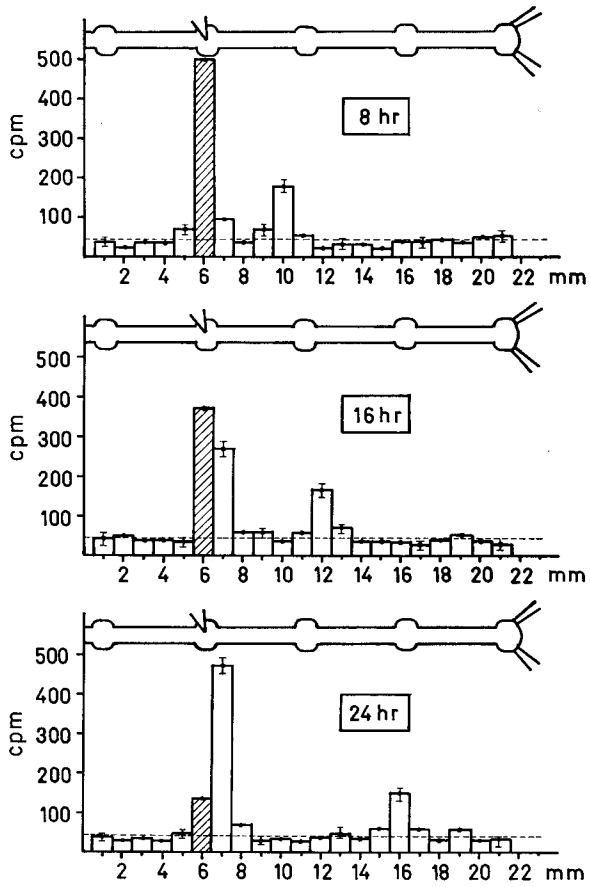

FIGURE 1 Representative distribution along the cord of leucine-^{3}H incorporated into TCA-precipitable protein. The animals were killed at the indicated times, and the radioactivity in each 1 mm segment of the cord was measured (*cpm*). Injected ganglia are marked with a *V* in the diagram of the cord. The counts in the injected ganglion are shown hatched and those of the background are indicated by the horizontal dashed lines. Two peaks can be observed, one proceeding at 1 mm/day and the other at 10 mm/day.

represent minimum transport velocities. Although transport velocities cannot be exactly calculated from radioautographs, the rates estimated here are consistent with those obtained from biochemical characterization of this system.

4 days after injection, when the slow protein component had moved 4 mm along the axons, the animal was killed and its nerve cord radioautographed. In this experiment, 4–7-μ serial cross-sections were made at 100-μ intervals along the interganglionic connective that contained the labeled protein. The results showed the label distributed within a 300–600 μ length of axon. One of these radioautographs is illustrated in Fig. 4 which shows explicitly that the migrating population of radioactive proteins move within the axons.

Vinblastine Treatment

In control nerve cords, when only leucine-^{3}H was injected, a peak of radioactivity was always detected moving caudad at 1 mm/day (Fig. 5 *a*). By contrast, when vinblastine was injected into the next ganglion behind the one into which leucine-^{3}H was administered 36 hr earlier, and the animal was killed 8 days later, the peak of radioactivity was not present in its normal position (i.e., 8 mm removed from the isotope-injected ganglion), but had moved only 1–3 mm (Fig. 5 *b*). When 16 days were allowed for transport, no label had passed the vinblastine-treated zone, nor had it accumulated at a ligature made close to the sixth abdominal ganglion (Fig. 5 *c*). Control tests with ligated cords, not treated with the drug,

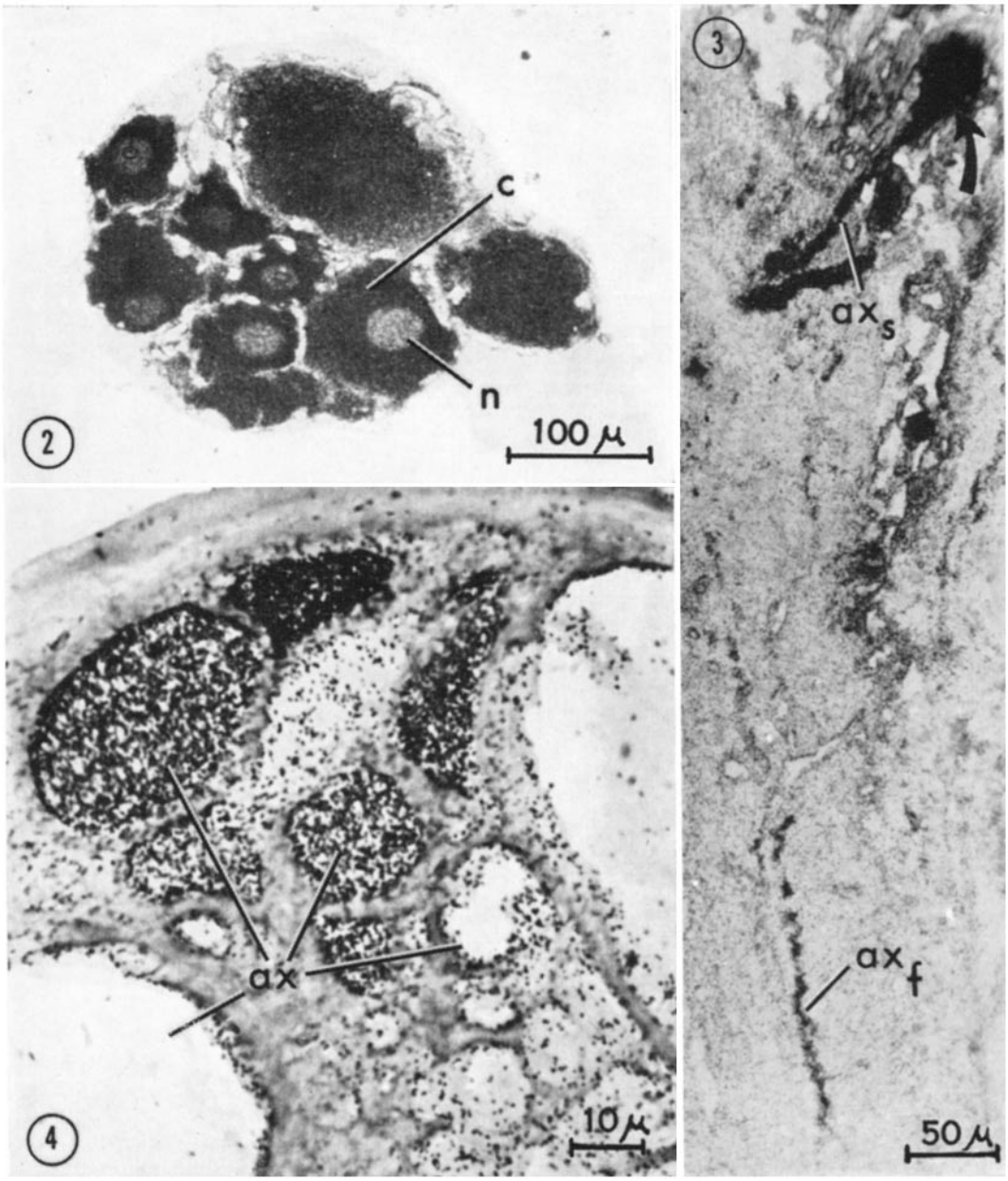

FIGURE 2 Radioautograph of section through a ganglion fixed 1 hr after injection of leucine-^{3}H. Silver grains are more concentrated over cytoplasm (*c*) as opposed to nuclei (*n*). × 720.

FIGURE 3 Distribution of grains in longitudinal section made 3 hr after leucine-^{3}H injection. Two labeled axons are indicated, one showing slow transport (ax_s) (perikarya indicated by arrow) and the other showing fast transport (ax_f). Estimated transport velocities are 1 mm/day and 10 mm/day (see text). × 100.

FIGURE 4 Radioautograph of cross-section of cord showing intraaxonal location (*ax*) of slowly transported protein-bound label. Section was made 4 mm distal to a ganglion injected with leucine-^{3}H 4 days earlier. × 1692.

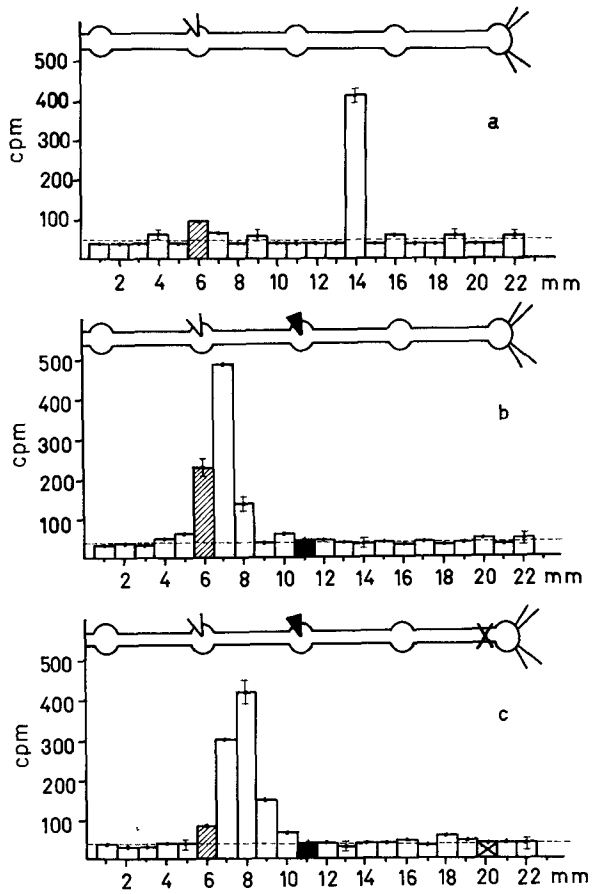

FIGURE 5 Distribution of tritium-labeled proteins in 1 mm segments along the nerve cord. Injected ganglia are marked with a *V*. Counts in the ganglion treated with leucine-^{3}H are shown hatched, and those in the ganglion treated with the drug are shown in black. In experiments with vinblastine, the drug was injected 36 hr after leucine-^{3}H. Background counts are indicated by the dashed lines. Experimental conditions: Fig. *5 a*, control animal killed 8 days after isotope administration. Peak is consistent with a rate of transport of 1 mm/day. Fig. *5 b*, animal injected with leucine-^{3}H and with vinblastine in adjacent ganglia and killed 8 days after the first injection. Transport is stopped proximal to ganglion injected with the alkaloid. Fig. *5 c*, same as Fig. *5 b*, but animal killed 16 days after treatment and ligature placed at point marked with an *X*. Transport is blocked, and no label accumulated at the ligature.

showed the expected accumulation of label at the proximal side of the ligature.

In 13 similar experiments, the isotope distribution was monitored at various time intervals following injections. The data obtained are summarized in Fig. 6, where the radioactivity resident in the leucine-injected ganglion, and that of the connective between injected ganglia, as well as total radioactivity, are plotted as related to the time between injection and death. In these experiments, the total amount of label proximal to the vinblastine-treated zone is not substantially different between experiments. Little or no protein-bound label moved beyond that ganglion treated with the drug for up to 17 days.

At the concentration used, vinblastine effectively blocked slow transport, but the aforementioned time interval between injections was not adequate to test the effect of the drug on fast transport. For the purpose of resolving this point, the alkaloid was injected (8–24 hr after the leucine-^{3}H) into the second ganglion posterior to the site of isotope application, and the animals were killed 3 days later. The results from 15 such experiments showed two peaks of labeled protein blocked by the action of vinblastine, one consistent with a rate of 1

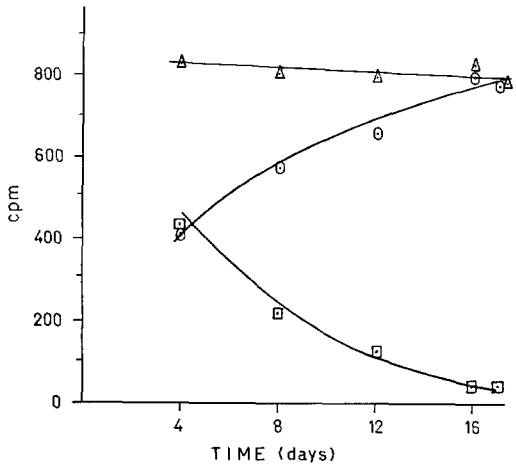

FIGURE 6 Data accumulated from 13 experiments in which vinblastine was injected (24 hr after leucine-^{3}H) into the next caudal ganglion from that to which the isotope was administered. Labeled protein resident in leucine-^{3}H-injected ganglion (⊡), in connective between injected ganglia (⊙), and the sum of both (△), are plotted as a function of the injection-to-death time interval (See text).

mm/day, and the other with a rate of approximately 10 mm/day (Figs. 7 *a*, 7 *b*). No signs of reversibility of the vinblastine-induced blockage were observed in similar experiments in which up to 16 days elapsed between injection of leucine and biochemical analysis.

The likelihood that some material moved rostrally, without being detected by our methods, was checked in a series of five experiments. In these tests, vinblastine was injected 24 hr after leucine-^{3}H into a ganglion located two ganglia rostrally from the site of injection of the isotope. The only movement detected was the slow transport directed caudad from the injected ganglion (Fig. 7 *c*).

Other aspects that define the effects of vinblastine on axonal transport were studied in a series of experiments. Four experiments involved vinblastine injections into the 2nd and 3rd ganglia caudal to that into which the isotope was administered. The fast and the slow peaks were blocked at the proximal side of the first vinblastine injection, whereas no label was found beyond the second vinblastine injection (Fig. 8 *a*). Subsequently, four experiments were completed involving injections of vinblastine into the 1st and 3rd ganglia posterior to the one that had been injected with leucine-^{3}H 24 hr earlier. These experiments showed blockage of slow transport in the connective between the isotope injection site and the site of first vinblastine injection, and of the fast transport in the segment between the two ganglia injected with the drug (Fig. 8 *b*). In six additional experiments, the alkaloid was injected 24 hr after leucine-^{3}H into the 3rd ganglion posterior to the site of isotope injection, and the animals were killed 3 days later. These particular tests showed that the drug blocked fast axonal transport but, because of the distances involved, did not block slow transport (Fig. 8 *c*). In four similar experiments, animals were killed 7 days (instead of 3 days) following vinblastine treatment, and the slow peak did not reach farther than 4–5 mm from the site of isotope injection (Fig. 9).

These and other experiments with the isotope and the alkaloid administered to the same ganglion have shown that the action of vinblastine extends from the site of application at least 8 mm (two interganglionic lengths) (Figs. 7 *a*, 7 *b*, and 8 *a*) but no more than 11 mm (F gs. 8 *c* and 9) along the cord.

Bioelectrical Activity

Vinblastine (0.1 and 0.2 mM), applied externally, had no effect on the bioelectrical activity of the nerve cord kept in vitro for up to 8 hr. For example, in 10 experiments the neural response to electrical stimulation of nerve cords treated with the drug could not be distinguished from that of control cords (Fig. 10). Furthermore, in four long-term experiments in which the drug was injected, in vivo, into one or more ganglia, vinblastine did not affect significantly the propagation of action potentials 5–8 days later (Fig. 10).

Electron Microscopy

Vinblastine caused loss of axonal microtubules and formation of characteristic intracellular aggregates only in ganglia from the 60 min experimental group (Figs. 11, 14). Such changes were not observed in axons or cell bodies in ganglia fixed 20 min, 4 days, 8 days, or 19 days after injection of the drug. However, a flocculent material not seen in control experiments was occasionally observed in axons from the 4-, 8-, and 19-day samples (similar to that seen in the lower part of Fig. 14).

Axons showing effects of vinblastine tended to be those near the point of injection of the drug.

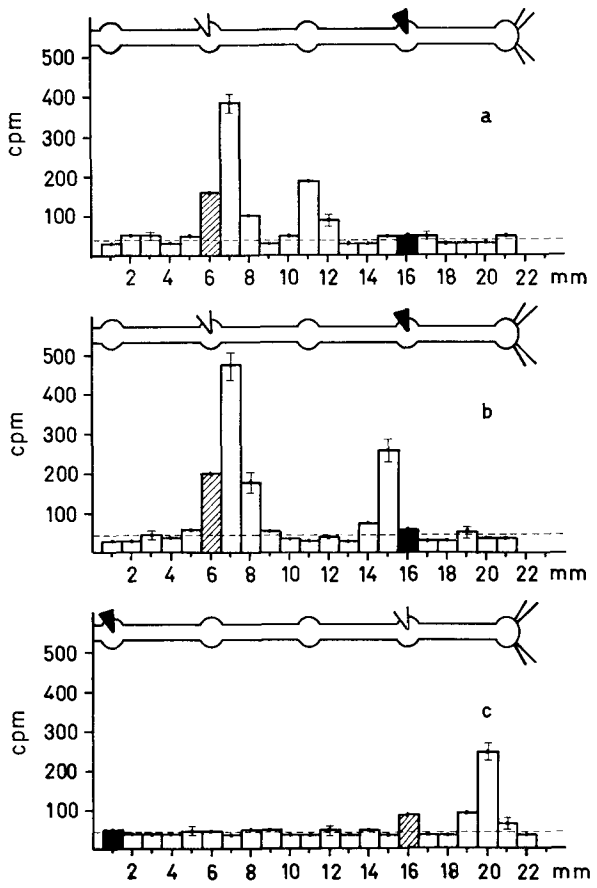

FIGURE 7 Same convention for symbols as in Fig. 3: leucine-^{3}H injection (hatched area), vinblastine injection (black), and background (dashed line). Experimental conditions: Fig. 7 *a*, animal injected with leucine-^{3}H 12 hr before vinblastine injection and killed 4 days after the first injection. Fast and slow transport are blocked. Fig. 7 *b*, same as Fig. 7 *a*, but the time between injections was 24 hr (instead of 12 hr). Fast and slow transport appear blocked. Fig. 7 *c*, same as Fig. 7 *a*, but vinblastine was injected into the ganglion located three ganglia anterior to the site of isotope injection.

Also, not all axons in a particular region were similarly affected. Fig. 14 shows two adjacent axons separated by flattened processes of supporting cells and two basal laminae. The upper axon in the figure appears relatively unaffected, while the lower axon is devoid of microtubules and contains aggregated material similar to that often seen in the midst of crystalloidal material.

In markedly affected axons, no microtubules are seen, and discrete masses of flocculent material are scattered in the axoplasm. On closer inspection, this aggregated material is found to have longitudinal or transverse periodicity, depending on the plane of section (Figs. 11, 12). The aggregated material seems to have the three-dimensional appearance of a honeycomb and in cross-section through the elements of the honeycomb one can see hexagonal profiles with a center-to-center spacing of 300 A (Fig. 12). This description is in keeping with previously reported descriptions of similar crystalloidal material induced by vinblastine (16, 24).

Axons affected by vinblastine sometimes contain mitochondria with dense and thickened membranes (Figs. 11, 13). In some cases, dense material appears as a thickened "plaque" associated with the membrane, as shown by the arrows in Fig. 13. Such altered mitochondria were noted only in axons or cell bodies containing crystalloidal elements and were never seen in control experiments.

Microtubules and mitochondria are the most

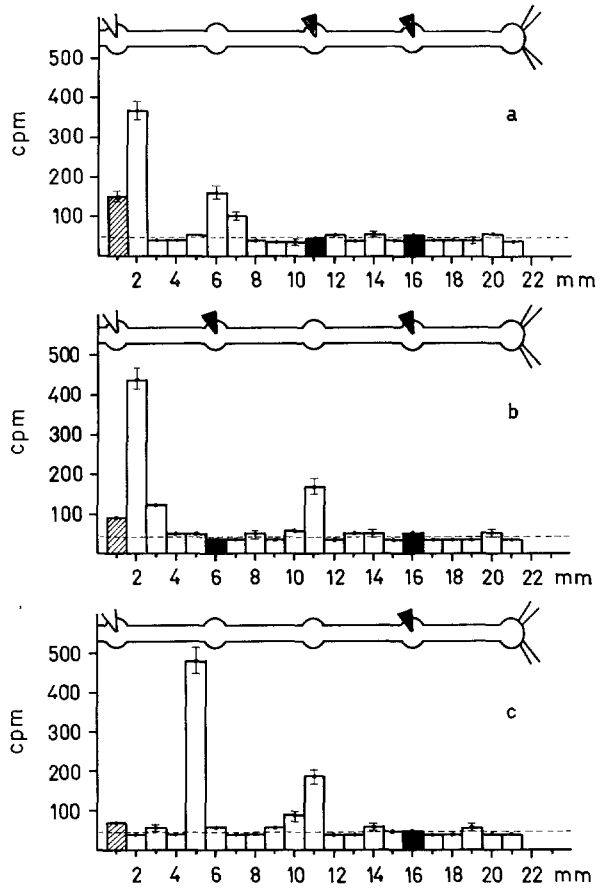

FIGURE 8 Same convention for symbols as in Fig. 7: leucine-^{3}H injection (hatched area), vinblastine injection (black), and background (dashed line). Experimental conditions: Fig. 8 *a*, animal injected with leucine-^{3}H 12 hr before vinblastine injection into the 2nd and 3rd ganglia posterior to that which received the isotope. The cord was dissected out 4 days after leucine-^{3}H administration. Fast and slow transport are blocked, and no label passed through the first block. Fig. 8 *b*, same as Fig. 8 *a*, but vinblastine was administered 24 hr after the isotope, into the 1st and 3rd posterior ganglia. Fast and slow transport are blocked; but the fast peak had passed the first posterior ganglion before vinblastine treatment. Fig. 8 *c*, animal injected with leucine-^{3}H 24 hr before vinblastine injection into the 3rd posterior ganglion. The cord was dissected out 4 days after isotope injection. Fast transport is blocked, but the slow peak is unaffected because after 4 days it is still outside the region of cord influenced by the drug.

prominent structures seen in axons of the crayfish nerve cord, and no structures were seen which could be classified as neurofilaments. Extending laterally from the surfaces of axonal microtubules, with which they appear to be associated, are wispy projections which can be resolved as filamentous elements (Fig. 15). These filamentous elements are about 40–80 A in diameter and vary in length up to 0.1 μ or so; sometimes they appear to branch or anastomose with neighboring elements associated with the same microtubule or with the surface of adjacent microtubules. In addition, the axoplasm appears to contain such filamentous material which is not associated with the surface of microtubules. Filamentous material was especially prominent in some axons from vinblastine-treated ganglia fixed 1 hr after injection. Portions of such axons often appear relatively "empty" owing to a decrease in the density of their matrix, and the few remaining microtubules often have filamentous masses associated with their surfaces which are irregularly aggregated and less "delicate" in appearance than those seen in control axons (Figs. 16, 17).

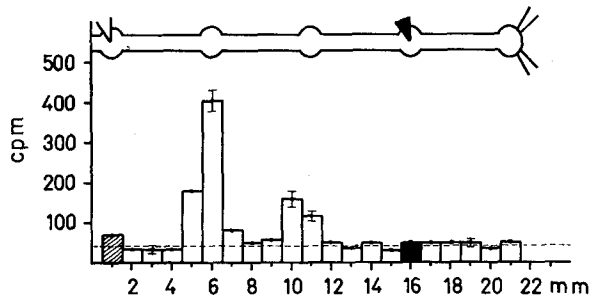

FIGURE 9 Same as Fig. 8 *c*, but the animal was killed 8 days after injection of the isotope. Both slow and fast peaks remained blocked.

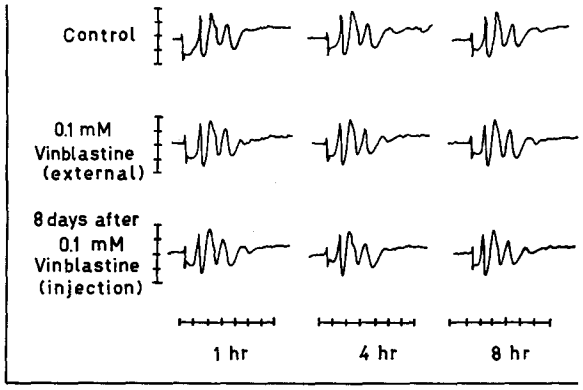

FIGURE 10 Bioelectrical activity of the nerve cord was monitored in vitro for up to 8 hr. In one case, vinblastine was added to the saline solution bathing the cord (*external*), and in another the drug was injected in the same manner as for the transport experiments (*injection*). The lower record illustrates the neural activity 8 days after the injection.

DISCUSSION

Rates of Transport

These experiments on the crayfish nerve cord show that axoplasmic proteins of perikaryal origin migrate distally within the axons at least at two rates, 1 mm/day and 10 mm/day. Similar transport velocities have been described by others (1–3). Recently, it has been shown that some axonal proteins are also transported at higher rates in the range of 100–500 mm/day (25–28). It is possible that these faster rates of transport also occur in the crayfish cord, but in the present study protein movements faster than 10 mm/day were not resolved. Our experiments were not designed to detect such fast rates; intervals shorter than 6 hr between injection and death would be required to resolve this point. Since the labeled neurons do not have processes in the rostral direction, the movement of proteins in this system was always caudad from the site of isotope injection, and no label was observed moving rostrally along the cord. Further, the sensory neurons directed rostrally have their perikarya in the periphery and not in the abdominal ganglia where the isotope was made available for incorporation into proteins.

The resolution of two distinct rates of transport, as contrasted with the one rate in a previous study (17), was achieved by the use of three times larger quantities of leucine-^{3}H and the sharp distribution maintained by the labeled material in its passage along the cord. Clearly, the rapid component with a 10-fold faster rate is different from that of the bulk displacement of the axoplasmic column moving at 1 mm/day. In addition, a comparison between the specific activity in each of the transported components indicates that the amount of protein-bound radioactivity in the fast peak is about half that of the slow peak. It was concluded earlier that a significant fraction of the labeled proteins moving at 1 mm/day reaches the end of

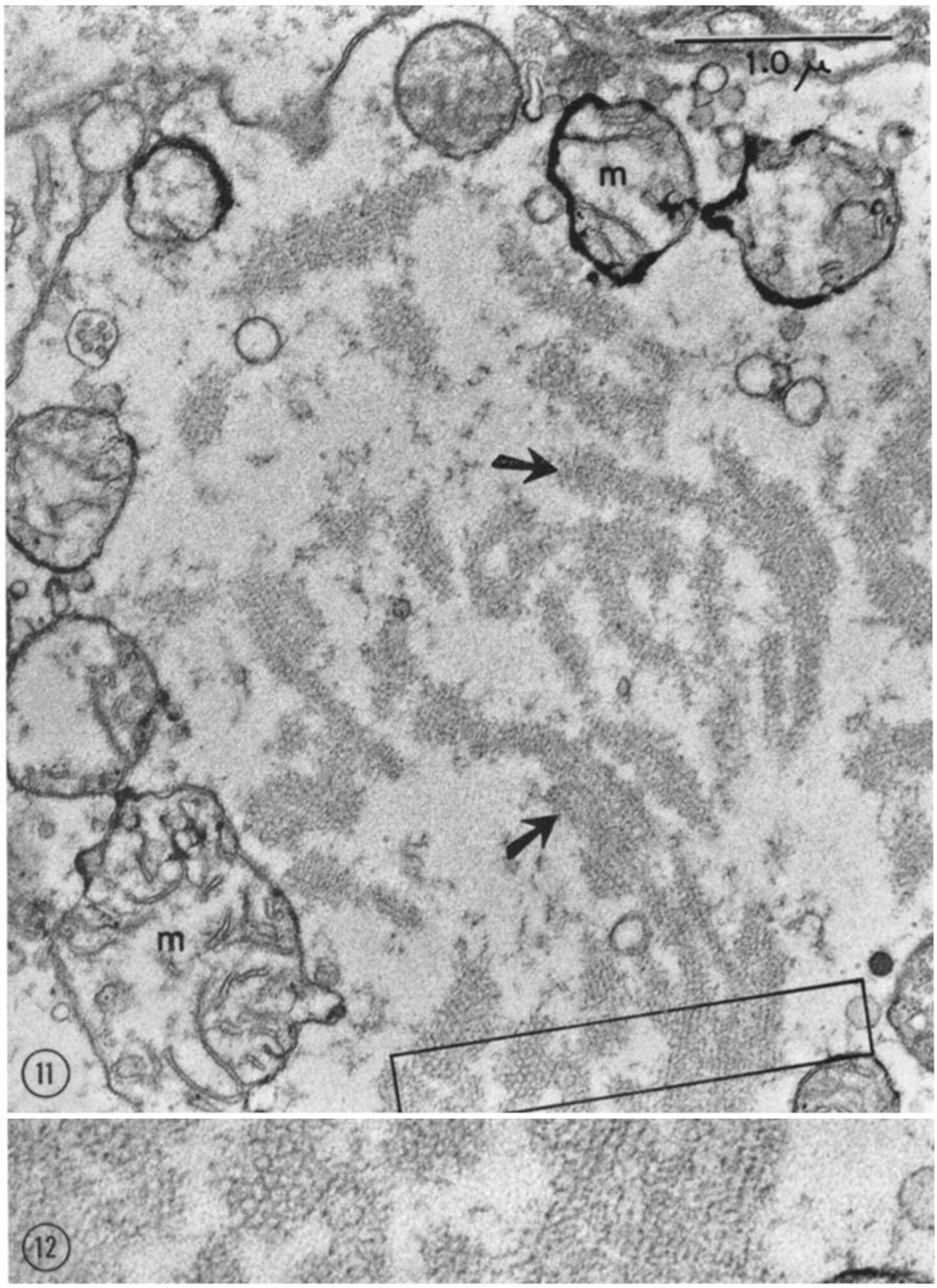

FIGURE 11 Transverse section through ganglionic axon showing effects of vinblastine treatment. Note masses of crystalloidal material (arrows), absence of microtubules, and dense material associated with some mitochondria (*m*). Rectangle shows portion enlarged in Fig. 12. × 31,800.

FIGURE 12 Enlarged portion of axoplasm shown in Fig. 11 showing repeat patterns seen in crystalloidal masses. Transverse section through hexogonal tubular profiles is seen at left of center, while longitudinal profiles are seen at right. × 63,600.

the axon (17). From the similarity in the patterns of decrease in the amount of label with distance along the cord, we can infer that a portion of the fast-moving protein component also reaches the terminus. The role played by these proteins that reach the terminal regions of the axon is still unknown, but the likelihood is that they may have importance in the trophic and transmitter functions of the nerve cells.

Whether the two components of transport detected are driven by the same or by different mechanisms is difficult to determine. At any rate, the linear displacement of the labeled peaks with time between injection and biochemical analysis suggests that the system(s) responsible for these transport processes must be present within and along the entire length of the axons. These and earlier studies (12, 17) show that the driving mechanism(s) for the translocation of proteins is not a simple diffusion phenomenon, nor a directed endoneurial fluid convection along diffusion gradients. In addition, the sharp localization of radioactivity and the absence of dispersion of the labeled protein suggest that the transported material is constrained from spreading, perhaps by some axonal structure involved in the mechanism(s) of axoplasmic movement. So far, the structures that have been proposed as probable candidates for such functions are the axonal membrane, microtubules, and neurofilaments. However, as pointed out in a recent discussion, it remains unclear which of these axonal constituents form the structural basis for the transport mechanism(s) (29).

Effects of Vinblastine Treatment on Axonal Transport

Vinblastine diffusing out from the injected ganglion effectively blocks the movement of the slow and the fast proteinaceous materials for a limited distance around the treated ganglion (up to 8–10 mm). The repressing action of this drug is due to a disruption of the transport system and not to inhibition of perikaryal protein synthesis (see Materials and Methods). Recently, it has been inferred that the protein subunits of the microtubules are transported mainly with the slow phase of axonal transport (1–2 mm/day) in the optic nerve of the goldfish (30) and in the crayfish nerve cord (12). This suggests that there is a dynamic equilibrium between the formed microtubules and local subunit pools in the axoplasm, as has been indicated in flagella elongation (31) and for ciliary proteins in the sea urchin (32). Hence, the binding of vinblastine to microtubule protein (15, 16) may upset the equilibrium between the associated and dissociated protein, thereby damaging the structural integrity of microtubules and interfering with the transport mechanism(s) which apparently require intact microtubules to function optimally.

At first sight, our findings appear to confirm the hypothesis that microtubules play a role in both slow and fast transport. This rationale is reinforced by the fact that colchicine interferes with fast transport of proteins (10, 11), acetylcholinesterase (9), and catecholamine storage granules (8) in mammals, and also with slow transport of proteins in the crayfish (12) and in the chicken (11). However, the irreversible blockage of transport for over 16 days is not easily explained by this interpretation since the effect of this drug on the structure of microtubules appears to be reversible in time (16, 33). Furthermore, exposure to vinblastine can interfere with transport without inducing complete loss of axonal microtubules, as discussed below.

Vinblastine-Induced Changes in Axonal Fine Structure

Although the prominent structural changes characteristic of vinblastine treatment were noted only in the 1-hr experiments (Figs. 11, 14) and in axons near the point of injection, there can be little doubt that the effects of the drug were more widespread and more subtle. Both fast and slow axonal transport were stopped completely up to 10 mm from the treated ganglion. Hence, the regions of the nerve cord in which transport was affected showed "intact" microtubules, and the effect of the drug on these structures was not necessarily concomitant with the blocking of transport. Disruption of microtubules and subsequent crystalloid formation may be a less subtle manifestation of vinblastine treatment. The blocking action of the drug without alteration of the gross morphology of microtubules is concordant with previous experiments in which slow transport was stopped by colchicine and cold for at least 10 days, while normal-appearing microtubules were observed by electron microscopy (12).

The formation of dense plaques on mitochondrial membranes indicates that microtubules

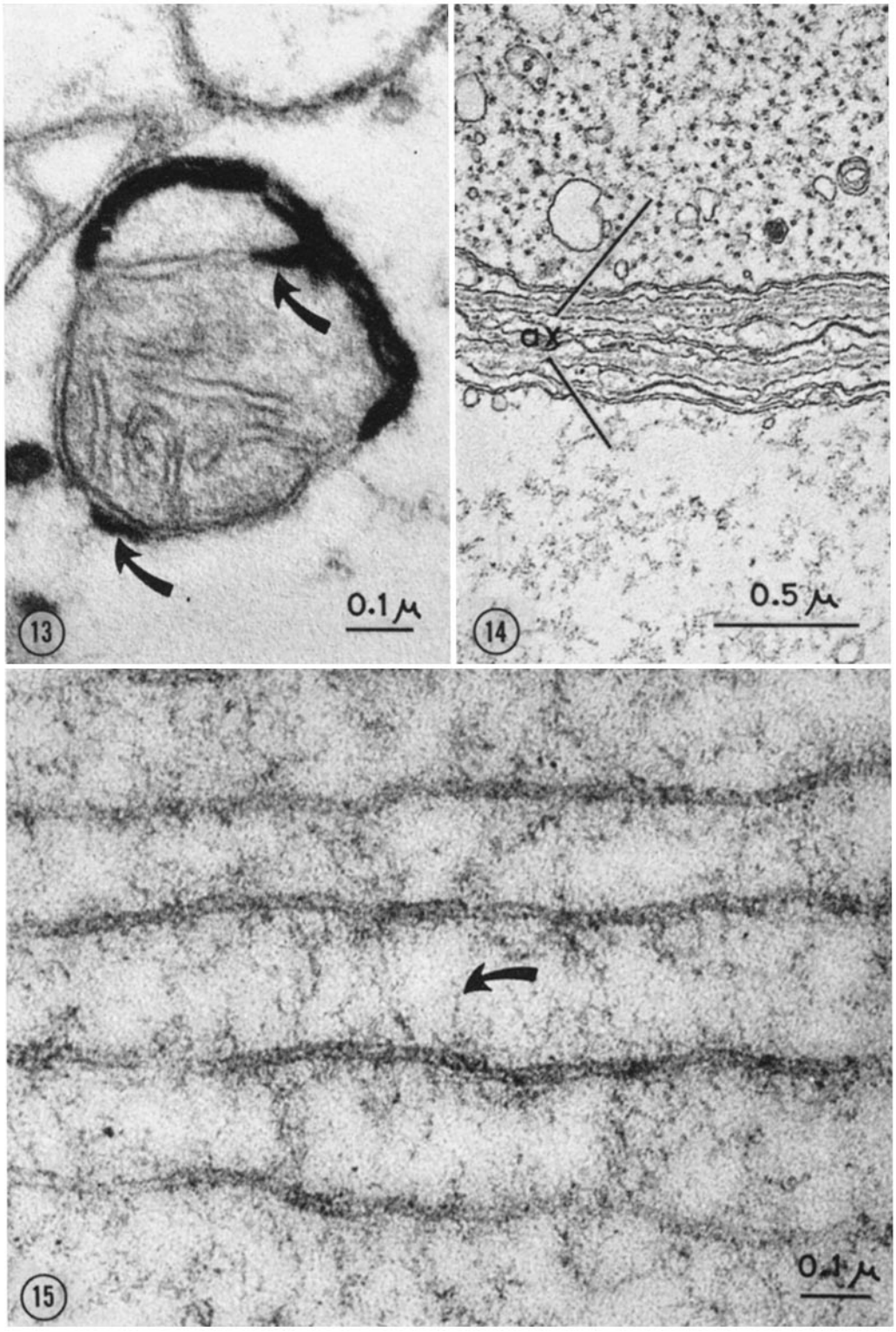
0.1 μ
13
0.5 μ
14
0.1 μ
15

are not the only structures affected by vinblastine. The effect on mitochondria needs further study. Nevertheless, the possibility exists that the arrest of transport by vinblastine resulted, at least in part, from interference with the oxidative function of mitochondria. In this connection, it has been reported that fast transport in mammalian nerves is closely dependent on oxidative metabolism (34).

We can infer that microtubules are implicated in transport only if it is assumed that vinblastine treatment had not dissociated all microtubules but had rendered them nonfunctional. This would mean that microtubules mediate both "fast" and "slow" transport. It must be recognized, however, that the drug may have blocked transport by interfering with other processes in addition to and independent of its action on microtubules.

Ultrastructural Basis of Axonal Transport

Axonal transport in the crayfish nerve cord cannot be attributed to neurofilaments, since they appear not to be present in this system. The possible roles of both microtubules and neurofilaments have been discussed recently (29), and at present there is no evidence to support the involvement of neurofilaments in axoplasmic transport.

If discrete structural elements are involved in transport in the crayfish nerve cord, one is obliged to focus attention on microtubules and the filamentous material associated with their surfaces and found in the axoplasmic matrix. As shown in Fig. 15, microtubules can become arranged in a highly regular manner to form channels lined with filamentous elements associated with their surfaces. In such arrangement, it is not certain whether microtubules act as the driving units supplying the motive power or whether they act passively as the structures that define only the pathway along which materials are transported (29). The first possibility has resulted in a speculative model regarding fast transport and has been discussed extensively (4, 5, 29). The second possibility leads us to hypothesize that the lateral filiform structures associated with the microtubules might be involved with propulsive mechanisms required for axoplasmic transport.

In this connection, such filamentous material appears to form a matrix in the axoplasm, both in control and in vinblastine-treated axons, similar to the networks of microfilaments in the growth cones and microspikes shown by elongating axons in culture (35). This fibrous material may serve a role in preserving the gelatinous integrity of the axoplasm, but the finding that the material is altered by vinblastine (Fig. 17) suggests that it may be a necessary component in the transport mechanism(s). Further, the persistence of the inhibition of transport over 16 days suggests that some durable vinblastine-binding site participates in axoplasmic movement. Such sites could be provided by the filamentous elements associated with the microtubules and/or the precursor material from which they may be assembled.

The authors are greatly indebted to Dr. P. F. Davison, Boston Biomedical Research Institute, Boston, Mass. for helpful discussion and constructive criticisms. We also thank Mrs. Maritza Fernandez for preparing the diagrams, and Mrs. Lorraine Hammer for excellent technical assistance.

This investigation was supported in part by Grant 01151-13 from the National Institute of Neurological Diseases and Stroke (to Dr. Samson), by Public Health Service Grant AI-06448 (to Dr. Burton), and by a United States Public Health Service Career Development Award 1-K3-GM-8620-01 from the Institute of General Medical Sciences (to Dr. Burton).

Received for publication 12 January 1971, and in revised form 16 February 1971.

FIGURE 13 Mitochondrion from an axon which contained crystalloidal elements induced by vinblastine treatment. Note dense material associated with inner (upper arrow) and outer (lower arrow) membranes. Material at bottom on outer membrane appears as a dense plaque. × 99,800.

FIGURE 14 Adjacent axons (*ax*) from vinblastine-treated nerve cord, one showing loss of microtubules and abundance of flocculent material while other appears relatively unaffected . × 28,000.

FIGURE 15 Longitudinal view of microtubules in axon of untreated nerve cord. Note spacing of microtubules and delicate lateral projections (arrow) associated with their surfaces. × 132,800.

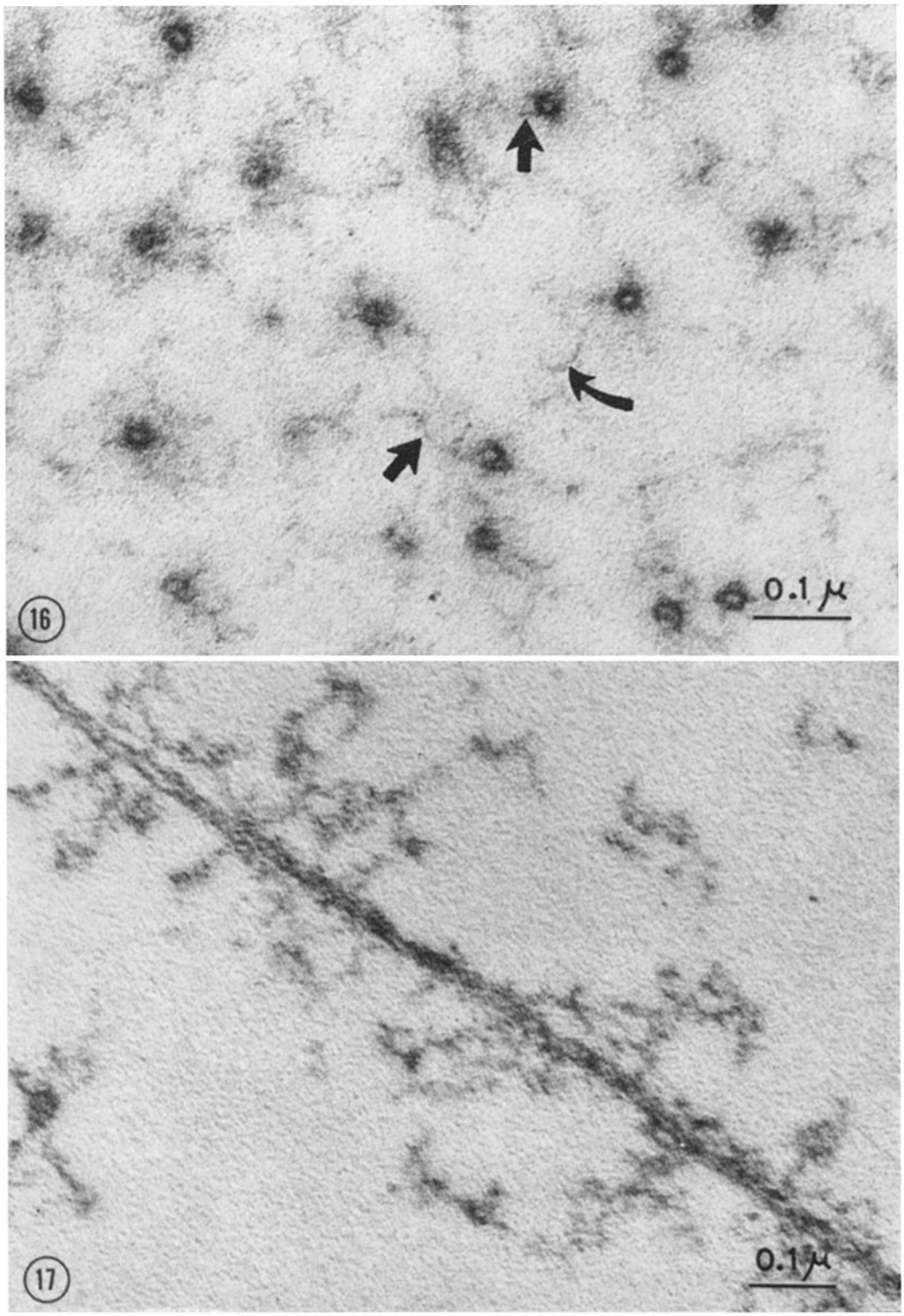

FIGURE 16 Transverse section of microtubles from axon of untreated nerve cord. Note short (upper straight arrow) and long (lower straight arrow) filamentous elements associated with surfaces of microtubules. Also note appareutly free filamentous elements in matrix of axoplasm (i.e., curved arrow). × 163,000

FIGURE 17 Longitudinal view of microtubule from axon showing prominent effects of vinblastine treatment. Not ecoarse lateral projections of microtuble and flocculent material in surrounding axoplasm, both commonly seen in such altred axons. × 132,800.

BIBLIOGRAPHY

1. Weiss, P. 1969. Neuronal dynamics and neuroplasmic (axonal) flow. *Symp. Int. Soc. Cell Biol.* **8**:3.
2. Barondes, S. H., and F. E. Samson. 1967. Axoplasmic transport. *Neurosci. Res. Program Bull.* **5**:307.
3. Grafstein, B. 1969. Axonal transport: communication between soma and synapse. *In Advanc. Biochem. Psychopharmacol.* **1**:11.
4. Schmitt F. O., and F. E. Samson. 1968. The molecular biology of neuronal fibrous proteins. *Neurosci. Res. Program. Bull.* **6**:119.
5. Schmitt, F. O. 1968. Fibrous proteins-neuronal organelles. *Proc. Nat. Acad. Sci. U.S.A.* **62**:1091.
6. Borisy, G. C., and E. W. Taylor. 1967. The mechanism of action of colchicine. *J. Cell Biol.* **34**:525.
7. Tilney, L. G., and J. R. Gibbins. 1969. Microtubules in the formation and development of the primary mesenchyme *Arbacia punctulata*. II. An experimental analysis of their role in development and maintenance of cell shape. *J. Cell Biol.* **41**:227.
8. Dahlstrom, A. 1968. Effect of colchicine on transport of amine storage granules in sympathetic nerves of rat. *Eur. J. Pharmacol.* **5**:111.
9. Kreutzberg, A. W. 1969. Neuronal dynamics and axonal flow. IV. Blockage of intra-axonal enzyme transport by colchicine. *Proc. Nat. Acad. Sci. U.S.A.* **62**:722.
10. Karlsson, J. O., and J. Sjöstrand. 1969. The effect of colchicine on the axonal transport of protein in the optic nerve and tract of the rabbit. *Brain Res.* **13**:617.
11. James, K. A. C., J. J. Bray, I. G. Morgan, and L. Austin. 1970. The effect of colchicine on the transport of axonal proteins in the chicken. *Biochem. J.* **117**:767.
12. Fernandez, H. L., F. C. Huneeus, and P. F. Davison. 1970. Studies on the mechanism of axoplasmic transport in the crayfish cord. *J. Neurobiol.* **1**:395.
13. Rodriguez Echandia, E. L., and R. S. Piezzi. 1968. Microtubules in the nerve fibers of the toad *Bufo arenarum* Hensel. *J. Cell Biol.* **39**:491.
14. Tilney, L. G., and K. R. Porter. 1967. Studies on the microtubules in heliozoa. II. The effect of low temperature on these structures in the formation and maintenance of the axopodia. *J. Cell Biol.* **34**:327.
15. Olmsted, J. B., K. Carlson, R. Klebe, F. Ruddle, and J. Rosenbaum. 1970. Isolation of microtubule protein from cultured mouse neuroblastoma cells. *Proc. Nat. Acad. Sci. U.S.A.* **65**:129.
16. Bensch, K., and S. Malawista. 1969. Microtubular crystals in mammalian cells. *J. Cell Biol.* **40**:95.
17. Fernandez, H. L., and P. F. Davison. 1969. Axoplasmic transport in the crayfish nerve cord. *Proc. Nat. Acad. Sci. U.S.A.* **64**:512.
18. Creasey, W. A., and M. E. Markiw. 1965. Biochemical effects of the Vinca alkaloids. III. The synthesis of ribonucleic acid and the incorporation of amino acids in Ehrlich ascites cells in vitro. *Biochim. Biophys. Acta.* **103**:635.
19. Karnovsky, M. J. 1965. A formaldehyde-glutaraldehyde fixative of high osmolarity for use in electron microscopy. *J. Cell Biol.* **27**:137A. (Abstr.)
20. Caulfield, J. 1957. Effects of varying the vehicle for osmium tetroxide in tissue fixation. *J. Biophys. Biochem. Cytol.* **3**:827.
21. Bennett, H. S., and J. H. Luft. 1959. *s*-Collidine as a basis for buffering fixatives. *J. Biophys. Biochem. Cytol.* **6**:113.
22. Reynolds, E. S. 1963. The use of lead citrate as high pH as an electron-opaque stain in electron microscopy. *J. Cell Biol.* **17**:208.
23. Kopriwa, B. M., and C. P. Leblond. 1962. Improvements in the coating technique of radioautography. *J. Histochem. Cytochem.* **10**:269.
24. Krishan, A., and D. Hsu. 1969. Observations on the association of helical polyribosomes and filaments with vincristine-induced crystals in Earle's L-cell fibroblasts. *J. Cell Biol.* **43**:553.
25. Ochs, S., and N. Ranish. 1969. Characteristics of the fast transport system in mammalian nerve fibers. *J. Neurobiol.* **1**:247.
26. Sjöstrand, J. 1970. Fast and slow components of axoplasmic transport in the hypoglossal and vagus nerves of the rabbit. *Brain Res.* **18**:461.
27. Karlsson, J. O., and J. Sjöstrand. 1968. Transport of labeled proteins in the optic nerve and tract of the rabbit. *Brain Res.* **11**:431.
28. Lasek, R. 1968. Axoplasmic transport in cat dorsal root ganglion cells: as studied with ^{3}H-leucine. *Brain Res.* **7**:360.
29. Davison, P. F. 1970. Microtubules and neurofilaments: Possible implications in axoplasmic transport. *Advanc. Biochem. Psychopharmacol.* **2**: 168.
30. Grafstein, B., B. S. McEwen, and M. L. Shelanski. 1970. Axonal transport of neurotubule protein. *Nature (London).* **227**:289.
31. Rosenbaum, J. L., J. E. Moulder, and D. L. Ringo. 1969. Flagellar elongation and shortening in *Chlamydomonas*. *J. Cell Biol.* **41**:600.
32. Auclair, W., and B. W. Siegel. 1966. Cilia regeneration in the sea urchin embryo: Evidence

for a pool of ciliary proteins. *Science (Washington)*. **154**:913.

33. MALAWISTA, S. E., H. SATO, and K. G. BENSCH. 1968. Vinblastine and griseofulvin reversibly disrupt the living mitotic spindle. *Science (Washington)*. **160**:770.
34. OCHS, S., and N. RANISH. 1970. Metabolic dependence of fast axoplasmic transport in nerve. *Science (Washington)*. **167**:878.
35. YAMADA, K. M., B. S. SPOONER, and N. K. WESSELLS. 1970. Axon growth: Role of microfilaments and microtubules. *Proc. Nat. Acad. Sci. U.S.A.* **66**:1206.